Water Research 273 (2025) 123024

Contents lists available at ScienceDirect

Water Research

journal homepage: www.elsevier.com/locate/watres

Energy production and denitrogenation performance by sludge biochar based constructed wetlands-microbial fuel cells system: Overcoming carbon constraints in water

Boda Ouyang [a,1], Zhiyong Zhang [c,1], Fuzhi Chen [a], Fei Li [a], Ming-Lai Fu [a,**], Huachun Lan [c], Baoling Yuan [a,b,*]

[a] Xiamen Key Laboratory of Municipal and Industrial Solid Waste Utilization and Pollution Control, College of Civil Engineering, Huaqiao University, Xiamen, Fujian 361021, PR China
[b] Key Laboratory of Songliao Aquatic Environment, Ministry of Education, Jilin Jianzhu University, Changchun, 130118, PR China
[c] Center for Water and Ecology, State Key Joint Laboratory of Environment Simulation and Pollution Control, School of Environment, Tsinghua University, Beijing 100084, PR China

ARTICLE INFO

Keywords:
Microbial fuel cell
Constructed wetland
Carbon limitation
Sewage sludge-biochar
Denitrifying bacteria

ABSTRACT

As freshwater demand grows globally, using reclaimed water in natural water bodies has become essential. Constructed wetlands (CWs) are widely used for advanced wastewater treatment due to their environmental benefits. However, low carbon/nitrogen (C/N) ratios in wastewater limit nitrogen removal, often leading to eutrophication. This study explores the use of sewage sludge biochar (SB) and activated carbon (AC) as electrodes in microbial fuel cell-constructed wetlands (MFC-CW) to enhance nitrogen removal and energy generation. Results indicated that the sludge biochar closed-circuit CW (MSBS-CW) achieved considerable total nitrogen removal (95.85 %) and maximum power density (9.05 mW/m^2). Furthermore, high-throughput sequencing and functional gene analysis revealed substantial shifts in the microbial community within MSBS-CW, particularly in the electroactive bacteria (*Geobacter*), autotrophic denitrifying bacterium (*Hydrogenophaga, Thiobacillus*) and anaerobic ammonium oxidation bacteria (*Candidatus_Brocadia*). Electrochemical and material characterization showed that SB enhanced the cathode's electrochemical performance and the anode's biocompatibility, thereby improving denitrification and energy generation. This study demonstrates that sludge biochar is an effective low-cost electrode material for MFC-CW systems, offering a sustainable solution for nitrogen removal and energy production under carbon-constrained conditions.

1. Introduction

As the global population grows and urban industrialization progresses, the demand for freshwater is increasing (Feng et al., 2023a). Recharging with reclaimed water from wastewater from treatment plants (WWTPs) is an effective way to address water scarcity (Liao et al., 2023). However, wastewater often contains higher levels of nutrients, especially nitrates (NO_3^-), and leads to eutrophication as directly discharging sewage without deep treatment (Wang et al., 2025; Wei et al., 2024). Generally, the deep treatments includes coagulation, adsorption, membrane separation, and advanced oxidation (Ouyang et al., 2024; Rashid et al., 2024; Venâncio et al., 2023). Nevertheless, the high

Abbreviations: CWs, Constructed Wetlands; WWTPs, Wastewater Treatment Plants; C/N, Carbon/Nitrogen ratio; SB, Sewage Sludge Biochar; AC, Activated Carbon; MFC, Microbial Fuel Cell; MSBS-CW, Microbial Fuel Cell with Sewage Sludge Biochar (Closed Circuit); MAC-CW, Microbial Fuel Cell with Activated Carbon (Closed Circuit); SBS-CW, Sewage Sludge Biochar Open Circuit Constructed Wetland; COD, Chemical Oxygen Demand; TN, Total Nitrogen; EEM, Excitation Emission Matrix; FT-IR, Fourier Transform Infrared Spectroscopy; XPS, X-ray Photon Spectroscopy; CV, Cyclic Voltammetry; DOM, Dissolved Organic Matter; ETSA, Electron Transfer System Activity; ORR, Oxygen Reduction Reaction; PARAFAC, Parallel Factor Analysis; PCR, Polymerase Chain Reaction.

* Corresponding author.
** Corresponding author at: Xiamen Key Laboratory of Municipal and Industrial Solid Waste Utilization and Pollution Control, College of Civil Engineering, Huaqiao University, Xiamen, Fujian 361021, PR China.
E-mail addresses: mlfu@hqu.edu.cn (M.-L. Fu), yuanbl@hotmail.com (B. Yuan).
[1] These authors contributed equally to this work.

https://doi.org/10.1016/j.watres.2024.123024
Received 6 September 2024; Received in revised form 19 December 2024; Accepted 20 December 2024
Available online 21 December 2024

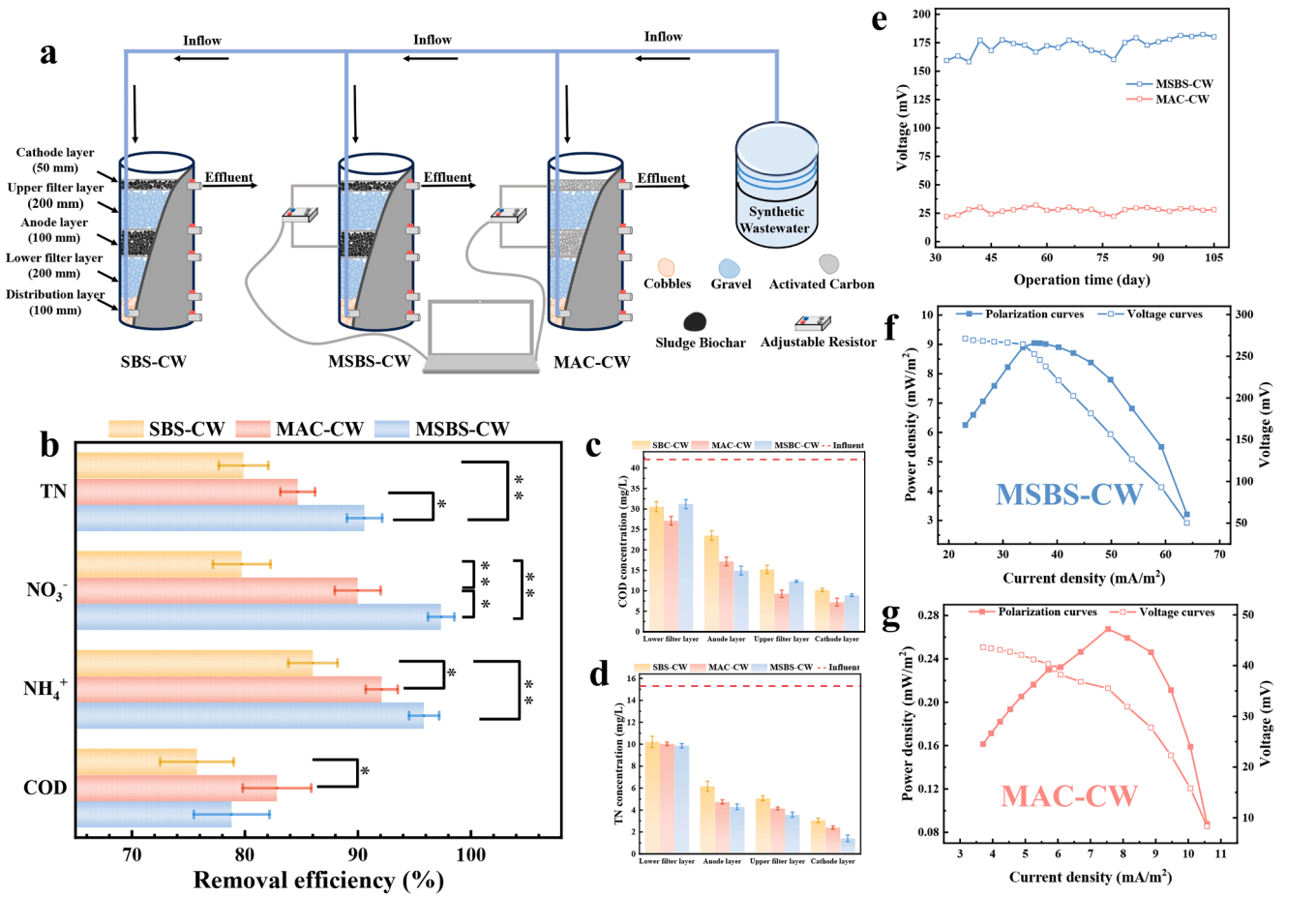

Fig. 1. (a) Schematic diagram of MFC-CW, (b) Different MFC-CW systems during the stabilization period pollutant removal efficiency, different depth concentrations of (c) COD and (d) TN, (e) operating voltage vary with time, polarization curves of (f) SB and (g) AC.

treatment costs and secondary pollution limit these technologies, making them unsuitable for long-term, stable treatment of reclaimed water (Feng et al., 2023b). Therefore, advanced wetland technologies capable of achieving deep nitrogen removal for reclaimed water are urgently needed.

Constructed wetlands (CWs) are nature-based wastewater treatment processes that have the characteristics of environmental friendliness, convenient operation and economy (Zheng et al., 2022). They convert pollutants through natural processes like biodegradation, adsorption, photodegradation, and phytoremediation, providing effective deep treatment of wastewater effluent. CWs could be classified into three categories of horizontal flow, horizontal submerged flow, and vertical submerged flow, in which vertical submerged wetlands have advantages like small area demand, suitable anoxic conditions, and high nitrogen removal capacity, making them suitable for NO_3^- removal (Zhao et al., 2024). However, previous research has investigated nutrient concentrations in effluents from 3340 WWTPs in China and found the average concentrations of chemical oxygen demand (COD) and total nitrogen (TN) were 33.8 mg l^{-1} and 10.9 mg l^{-1}, respectively (Sun et al., 2016). In addition, NO_3^- removal heavily relies on biological heterotrophic denitrification in CWs under anoxic conditions, using organic matter as an electron donor (Pyo et al., 2024). The low carbon/nitrogen (C/N) ratio in wastewater is inadequate for complete denitrification in CWs.

Recently, the various methods to enhance nitrogen removal in CWs, including adding plant litter (Zhou et al., 2024), fermentation broth (Chen et al., 2022), biochar (El Barkaoui et al., 2023), and pyrite (Yan et al., 2021), have been extensively studied. Among these, biochar has gained significant interest as a carbon-rich product from anaerobic, high-temperature biomass treatment (Zhuang et al., 2022). Previous studies have shown that adding biochar to CW-treated secondary effluent could significantly improve nitrate-N removal (Guo et al., 2023a). Guo et al. investigated the nitrogen removal efficiency when using biochar as a CW substrate and found that it could enrich genes encoding nitrate metabolism enzymes (Guo et al., 2023b). Zheng et al. prepared biochar from cattail and sewage sludge for CW, in which the release of dissolved organic matter (DOM) and higher electron transfer capacity of sewage biochar (SB) obviously enhanced nitrogen removal (Zheng et al., 2022). In addition, the anaerobic ammonium oxidation activity for denitrification could be significantly stimulated (Wang et al., 2022a).

Moreover, the high electrical conductivity, electron-donating ability, and biocompatibility likely make biochar has been deemed to an ideal electrode material for microbial fuel cells coupled with constructed wetlands (MFC-CW). The electrons were generated by microorganisms oxidizing organic matter at the anode, and move along an external circuit to the cathode and bind to electron acceptors (e.g., NO_3^-) (Gupta et al., 2023). In addition, MFC-CW could enhance nitrogen removal by improving the abundance and diversity of microbial communities (Xu et al., 2018). MFC-CW has been considered as a promising method for simultaneous nitrogen removal and power generation. Commercial electrode materials commonly used in MFC-CW studies include carbon cloth, carbon felt, and activated carbon, which are effective due to their high specific surface area and electrical conductivity (R. Lu et al., 2024; Yang et al., 2022). However, their high-cost limits practical applications. In contrast, sludge biochar, produced by pyrolyzing sludge, is a low-cost conductive material (Mian et al., 2019). Moreover, graphitic-N and pyridinic-N could be produced during sludge biochar pyrolysis, facilitating electrical activation and redox processes (Mian et al., 2022). It

was favoring the oxygen reduction reaction (ORR) and denitrification processes at the cathode. Previous studies have shown that sewage biochar anode could improve the power output of MFC due to the biocompatibility and slow-release carbon source (Feng et al., 2018; Zhu et al., 2022a). Table S1 compares the power densities reported for other MFC-CWs (Ji et al., 2022; Tang et al., 2019; Tao et al., 2022a; Zhang et al., 2024a). Notably, Zhang et al. obtained the highest power density of 44.64 mW m^{-2} using sewage sludge biochar as the MFC-CW electrode material (Zhang et al., 2024a). However, the energy production and denitrification performance in carbon constraint constructed wetlands-microbial fuel cells system are still unknown, and further research is needed. The feasibility of sewage biochar as a low-cost carbon-based electrode in MFC-CW for treatment low carbon/nitrogen (C/N) ratio wastewater, which will provide a new way for municipal sludge treatment.

Therein, the nitrogen removal and electricity production performances of MFC-CW using commercial activated carbon (AC) and sewage sludge biochar (SB) as electrodes were compared. The objectives of this study are (i) to explore the feasibility of sewage sludge biochar as carbon-constrained MFC-CW electrodes, (ii) to investigate the enhancement mechanisms based on the surface properties of the materials, and (iii) to examine the synergistic effect of combining SB and MFC regarding enhanced nitrogen removal and energy production. The obtained results showed that sludge biochar closed circuit CW (MSBS-CW) effectively enhanced power production and nitrogen removal efficacy, providing a reference method for recycling waste biomass and constructing wetlands for reclaimed water deep treatment.

2. Materials and methods

2.1. Substrate preparation

Sewage sludge was collected from a wastewater treatment plant (Xiamen, China) and converted into biochar using modified methods based on previous research (Zhang et al., 2024b; Zheng et al., 2022). The retrieved sludge was dried at 105 °C to constant a weight, and then flattened and sieved. After that, the sludge was pyrolyzed in a tube furnace under nitrogen at 600 °C for two hours to obtain sludge biochar (1–3 mm). Gravel (2–4 mm diameter) and pebbles (4–6 cm diameter) were purchased from Gongyi Gravel Factory (Henan, China), while activated carbon (2–4 mm diameter) was obtained from a Bafang Water Purification Plant.

2.2. Construction and operation of CW

Three sets of laboratory-scale CW microcosms were established, as shown in Fig. 1a, of sludge biochar-based CW (SBS-CW), closed-circuit sludge biochar-based CW (MSBS-CW), and closed-circuit activated carbon-based CW (MAC-CW). Each system was constructed using polymethyl methacrylate (inner diameter 180 mm, height 750 mm) and divided into five layers of 100 mm water distribution layer (cobbles), 200 mm lower filter layer (gravel), 100 mm anode layer (AC or SB), 200 mm upper filter layer (gravel), and 50 mm cathode layer (AC or SB). Besides, the cathode and anode were prepared according to previous methods (Ji et al., 2022), compacted with AC or SB, and wrapped in stainless steel mesh (SSM). The two electrodes were connected to an external adjustable resistor (0.1–15000Ω) using insulated copper wire with epoxy glue applied to prevent corrosion at the connection points. The CW influent was synthetic wastewater (COD = 40 mg l^{-1}, NO_3^--N = 13 mg l^{-1}, NH_4^+-N = 2 mg l^{-1}, TP = 0.4 mg l^{-1}, pH = 7.4 ± 0.2) configured according to previous study, and the specific compositions were listed in Table S2 (Sun et al., 2016). In addition, the hydraulic retention time was set to 3 days, and microorganisms in CW were inoculated using sludge from a sewage plant biochemical tank. Before the experiment, the microorganisms in CW were acclimated and cultured with synthetic wastewater until the effluent pollutant concentration stabilized.

2.3. Sample analysis and material characterization

Influent and effluent samples were collected every 3 days, filtered through a 0.45 μm membrane, and immediately analyzed for COD, nitrate nitrogen (NO_3^--N), ammonia nitrogen (NH_4^+-N), and total nitrogen (TN) using a UV–Vis spectrophotometer (DR6000, HACH, USA). Effluent from different functional layers was collected and examined on days 15 and 60 at steady state to explore water quality changes along the pathway. Real-time voltage was automatically collected every 2 min using an eight-channel voltage detection unit (Sin-R5000C, China). Polarization and power density curves were measured by varying external resistance values. Electrochemical indicators such as output power (P, mV), current (I, mA), power density (PD, mW m^{-2}), and current density (CD, mA m^{-2}) were calculated from the output voltage. Detailed calculations were provided in Text S1. Additionally, DO and pH were measured in situ using portable instruments. The heavy metals were measured using inductively coupled plasma mass spectrometry (ICP-MS, Agilent 7800).

Surface morphological features were analyzed by scanning electron microscopy (S-4800, Hitachi), and surface elements were determined by energy dispersive spectroscopy (EDS). Surface functional groups were identified using a Fourier transform infrared spectrometer (Nicolet iS10, Thermo) in the wave number range 400 - 4000 cm^{-1}. Surface elemental species were analyzed using X-ray photon energy spectroscopy (K-alpha, Thermo). Brunauer-Emmett-Teller (BET) surface area and pore volume were measured using ASAP 2460 (Micromeritics). Crystallinity information was obtained using a Raman spectrometer (alpha300R, WITec). CV curves were used to interpret the electrochemical properties of the materials and were measured using an electrochemical workstation (Chi660e, Shanghai Chenhua) according to previous methods (Text S2). DOM was extracted under neutral 20 °C deionized water conditions, and DOC concentration was measured using an organic carbon analyzer (TOC-L, Shimadzu). Filtered samples were analyzed by absorption spectroscopy and fluorescence excitation-emission matrix (EEM) using a fluorescence spectrometer (F-7100, Hitachi). Parallel factor analysis (PARAFAC) was performed on the EEM data after background subtraction. In addition, the electron transfer activity (ETSA) of each system was determined as described in Text S3.

2.4. Microbial communities and genes relative abundance

Substrate samples were collected from the MFC-CW anode and air cathode layer, then shaken and centrifuged to separate the biofilm. The samples were stored at −80 °C until DNA extraction. Gene V3-V4 fragments were amplified from extracted DNA using primer sets 515F (5′-GTGYCAGCMGCCGCGGTAA-3′) and 806R (5′-GGACTACNVGGGGTWTCTAAT-3′) and analyzed by high throughput sequencing. In addition, nitrogen metabolism-related genes were quantified using quantitative PCR (qPCR). Primers were derived from previous studies and the relative abundance of genes was calculated by absolute copies in 16S rRNA (Zhou et al., 2022).

2.5. Data analysis

All experiments were repeated, and the mean and variance were calculated. Pollutant removal efficiency was assessed by calculating the mean concentration, with data collected every 3 days during the stabilization period (0 – 105 days). SPSS (version 26.0) was used for statistical analysis. Additionally, one-way analysis of variance (ANOVA) was used, with $p < 0.05$ considered statistically significant.

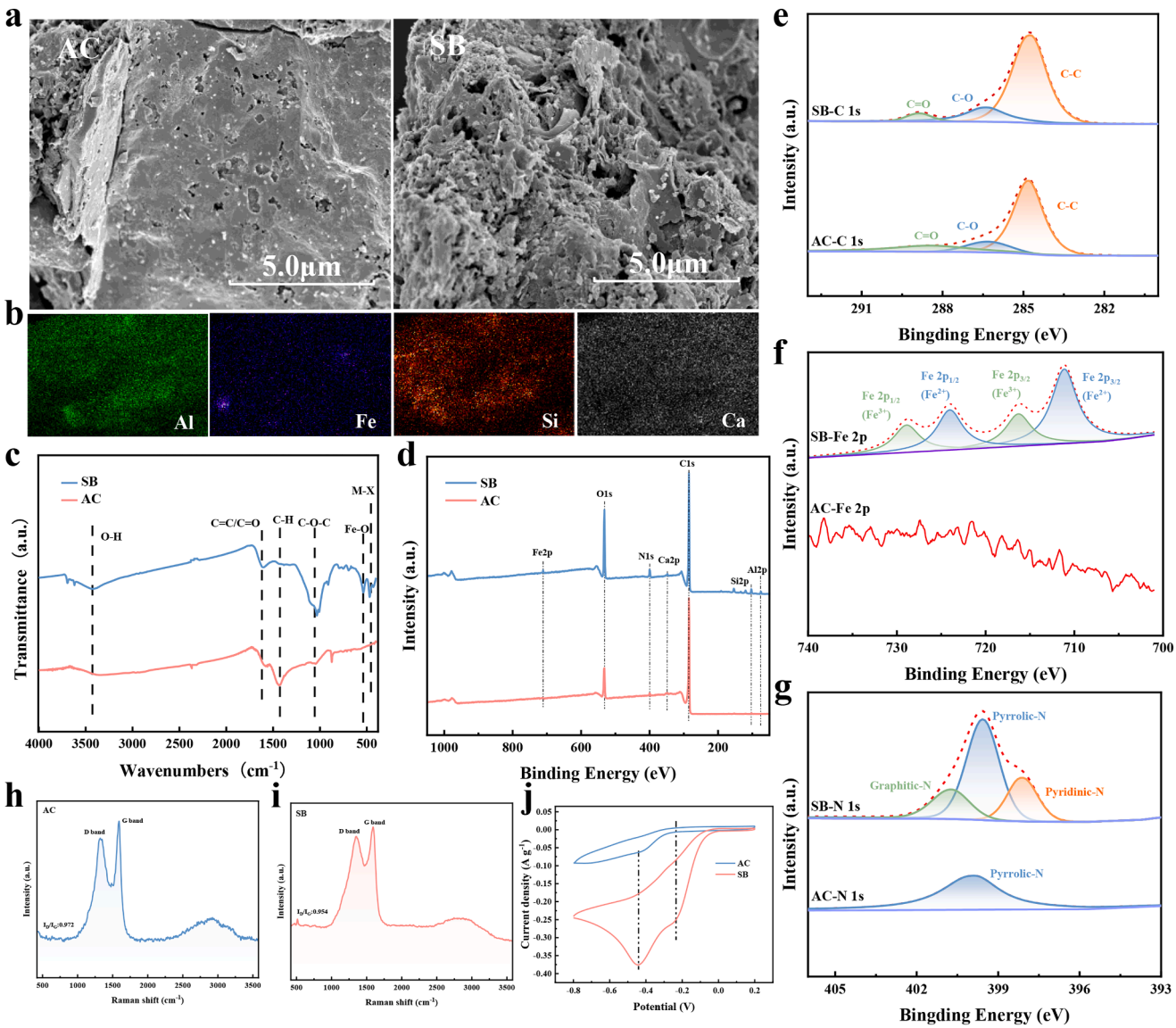

Fig. 2. SEM images of (a) SB and AC, (b) EDS image of SB, (c) FT-IR spectra, (d) full XPS spectra, (e) C 1 s spectra, (f) Fe 2p spectra, (g) N 1 s spectra, Raman spectra of (h) AC and (i) SB, and (j) CV curves for both materials.

3. Results and discussion

3.1. Treatment performance of constructed wetlands

3.1.1. Chemical oxygen demand and nitrogen removal performance

Figs. S1–S3 presented the influent and effluent pollutant concentrations and removal efficiencies for each CW group during the stabilization period, demonstrating stable pollutant removal over long-term operation. Additionally, Fig. 1b displays the treatment performance of different wetlands. The COD removal at SBS-CW, MSBS-CW and MAC-CW were achieved 75.76 %, 78.82 % and 82.84 %, respectively. MAC-CW had high COD removal due to the larger specific surface area of the activated carbon, which was facilitated to microorganism attachment and growth (Ji et al., 2022). The sludge biochar MFC-CW system exhibited higher COD removal than the CW system, consistent with previous studies (Tao et al., 2024; Xu et al., 2018). Understanding the COD removal process is critical because it serves as a substrate for nitrogen removal and MFC power generation (Zhang et al., 2024a). Therefore, COD concentrations at different depths were examined (Fig. 1c). It was observed that MAC-CW had a low COD concentration in the lower filter layer. Conversely, MSBS-CW had a low COD concentration in the anode layer, indicating substantial consumption of organic matter for electricity production (Teoh et al., 2024). Additionally, most organic matter was degraded at the bottom of the reactor, suggesting that microbial metabolic activities primarily utilized the organic matter as electron donors for nitrate reduction and energy production.

For NH_4^+ removal, as shown in Fig. 1b, SBS-CW achieved 86.01 % efficiency, while MAC-CW and MSBS-CW demonstrated higher efficiencies of 92.10 % and 95.85 %, respectively. This is likely due to the higher abundance of ammonifying bacteria in MAC-CW and MSBS-CW (Zhu et al., 2022b). Besides, the NO_3^- removal efficiencies for SBS-CW, MAC-CW, and MSBS-CW were 79.72 %, 89.98 %, and 97.37 %, respectively. The denitrification process was an electron-driven biochemical reaction that could be facilitated by the surface groups of SB and AC through modulation of electron transfer (Zhang et al., 2024a). Notably, the closed SB system significantly improved the denitrification process, likely due to bioelectricity promoting microbial structure and electron transfer (Liu et al., 2023). Interestingly, trends in nitrogen and COD removal were inconsistent. The conventional denitrification carbon source was a limiting factor and became more challenging under reclaimed water carbon-limiting conditions. It was indicated the

presence of alternative denitrification processes, such as autotrophic denitrification or anaerobic ammonium oxidation in the MSBS-CW system (Tao et al., 2022a). Besides, TN concentrations at different depths were examined (Fig. 1d). At the anode layer, MSBS-CW and MAC-CW removed high TN of 5.56 and 5.29 mg l^{-1}, respectively. The MFC-CW enhanced TN removal might be attributed to the higher number of NO_3^- reducing bacteria (Li et al., 2024). Furthermore, MSBS-CW removed the high amount of TN (2.16 mg l^{-1}) in the cathode layer might due to NO_3^- being available for autotrophic nitrogen reduction at the cathode electronic stimulation (Gupta et al., 2023). NO_2^- significantly threatens the environment and ecosystems. Fig. S4 presented the residual NO_2^- concentrations for each system, with values of 0.40 ± 0.15 mg $l^{-1}$for SBS-CW, 0.45 ± 0.15 mg l^{-1} for MSBS-CW, and 0.32 ± 0.11 mg l^{-1} for MAC-CW. These results suggested that each system could totally remove nitrogen and have less impact on the environment.

3.1.2. Energy generation performance

The voltage curves of MSBS-CW and MAC-CW over time was showed in Fig. 1e. During the stabilization period, MSBS-CW exhibited a 6.4-time higher voltage (172.46 ± 6.80 mV) compared to MAC-CW (26.96 ± 3.25 mV). This indicated that SB was more favorable for enriched electroactive bacteria (EAB) for power generation (Ebrahimi et al., 2021). The power density was calculated by varying the external resistance value, as shown in Fig. 1f and g. The outcomes showed that the maximum power densities of MSBS-CW and MAC-CW were 9.05 mW m^{-2} and 0.27 mW m^{-2}, respectively. Previous studies suggest that biochar is an ideal anode material due to its electron-donating capacity and excellent biocompatibility (Feng et al., 2018; Zhu et al., 2022a). Moreover, higher contents of N, Fe, and P enhance the ORR catalytic activity of the air cathode (Yuan et al., 2015). It was indicated that sewage sludge biochar is an excellent material for both cathode and anode applications in carbon-constrained conditions. Table S1 compares the power densities reported for other MFC-CWs and the highest power density of 44.64 mW m^{-2} using sewage sludge biochar as the MFC-CW electrode material (Ji et al., 2022; Tang et al., 2019; Tao et al., 2022a; Zhang et al., 2024a). Therein, the limitation of COD (40 mg l^{-1}) in this study was resulted in less electron transfer at the anode (Tao et al., 2022b).

3.2. Characterization of electrode materials

SEM of SB and AC was showed in Fig. 2a. The surface of SB was rough and mainly composed of amorphous and carbon particles, facilitating microorganism attachment and growth. In contrast, AC had smoother surfaces with numerous tiny pores. The EDS image of SB had detected elements such as C, O, Fe, Al, Si, and Ca, which were evenly dispersed on the surface (Figs. 2b and S5). Meanwhile, Fe could be acted as an electronic mediator for autotrophic denitrification, and N-coordinated Fe exhibits high catalytic activity for ORR (Yuan et al., 2015). Previous studies have shown that heteroatom doping enhances the catalytic activity of biochar (Wang et al., 2022b). Furthermore, the concentrations of heavy metals in both reactors and SB immersed in pure water were minimal (Table S3), indicating that releasing heavy metals from SB

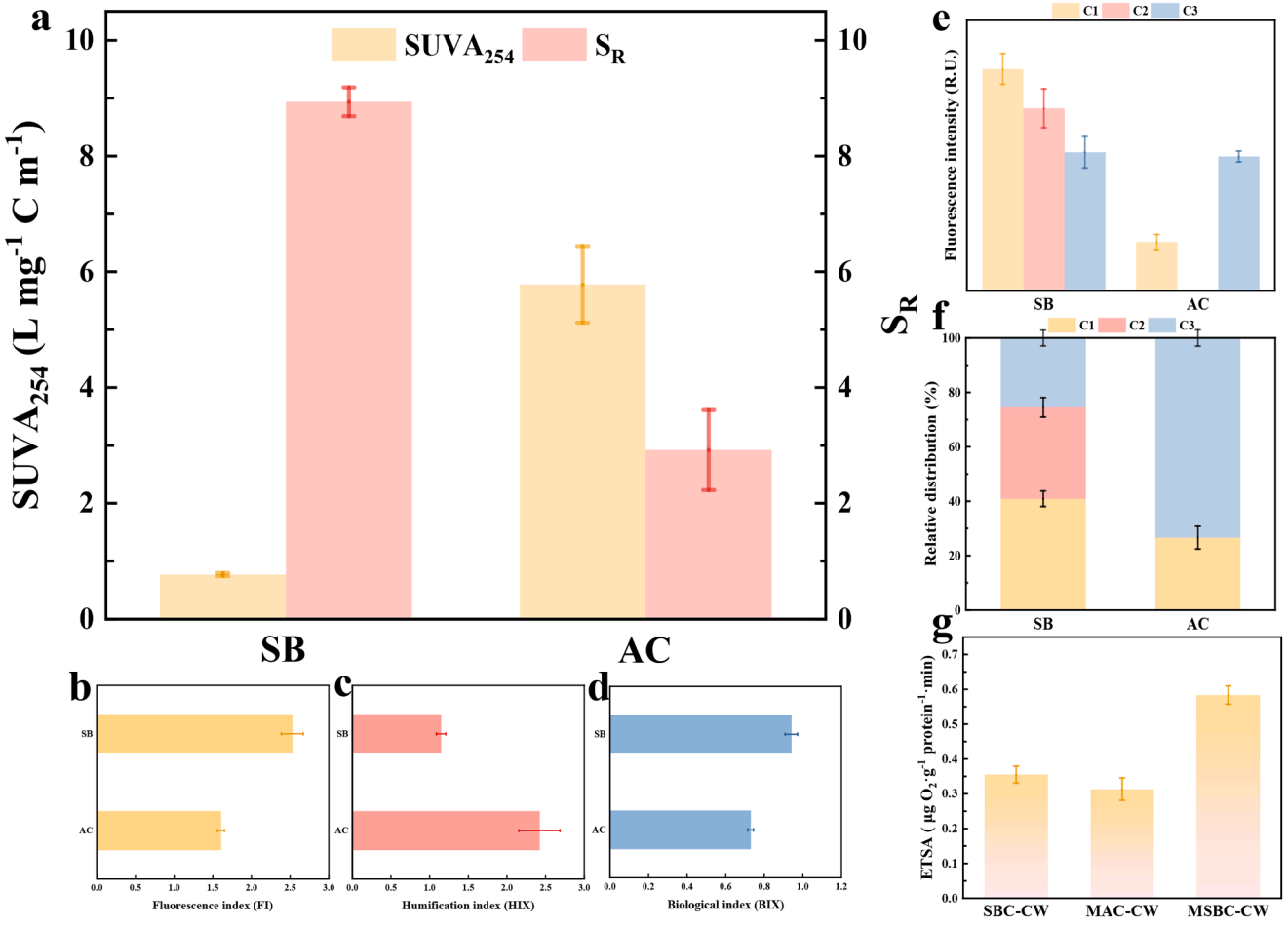

Fig. 3. (a) $SUVA_{254}$ and S_R values for DOM released from carbon materials, EEM (b) fluorescence index, (c) humification index, (d) biological index, (e) fluorescence intensity and (f) relative distribution of different components (C1 - C3 represent component 1 - component 3, respectively), and (g) different MFC-CW cathode microbial electron transfer activity.

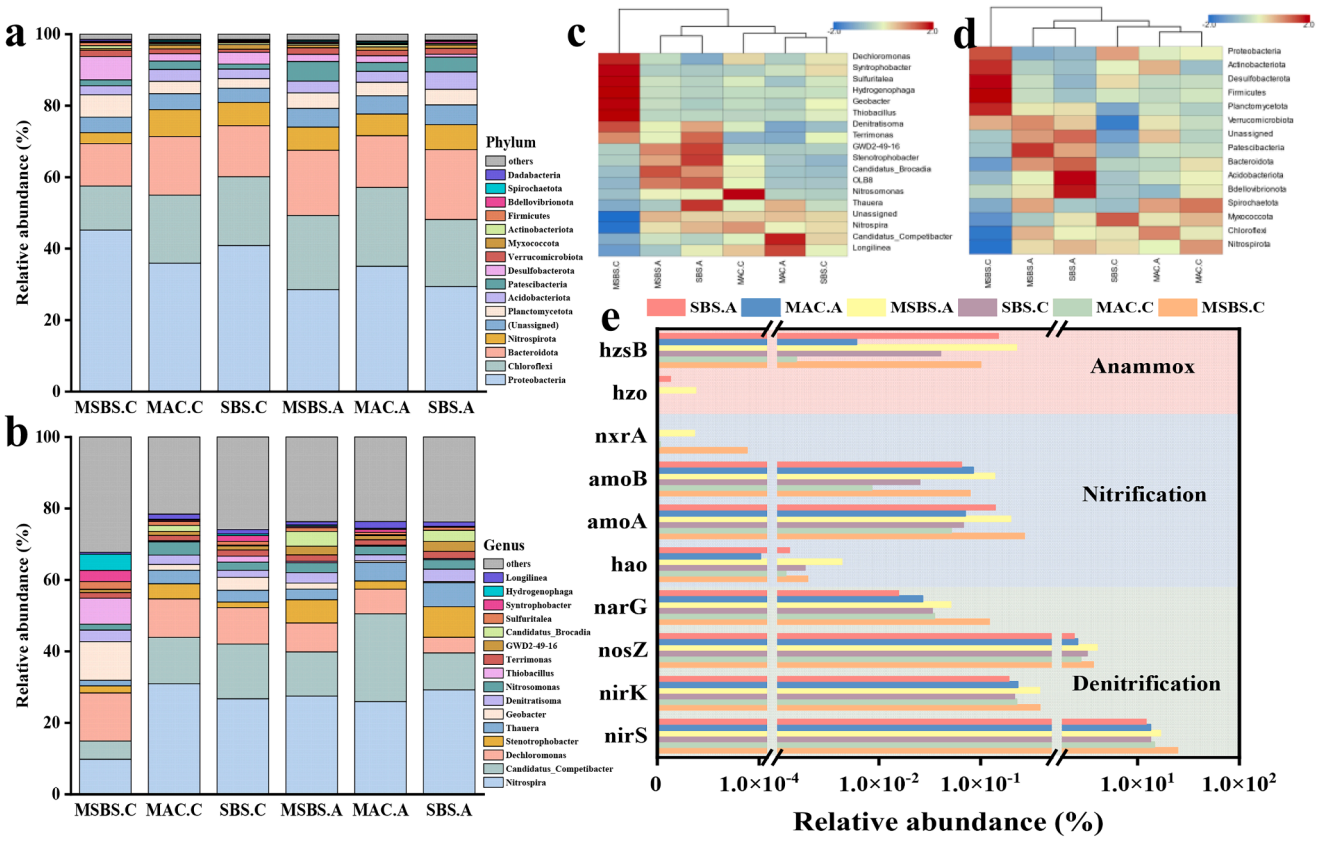

Fig. 4. Community structure of microbial communities at the (a) phylum and (b) genus levels, and clustering results at the (c) phylum and (d) genus levels, and (e) relative abundance of nitrogen functional metabolism genes, with A and C representing the anode and cathode area samples, respectively.

poses negligible environmental risk.

The surface functional groups of the electrode materials were characterized by FT-IR, as shown in Fig. 2c. The O-H stretching vibrations generated the broad peak at 3428 cm^{-1}, which was more prominent in SB. Previous studies have shown that phenol-OH groups could actively participate in electron transfer during nitrate and nitrite reduction processes (Zheng et al., 2022). The peaks at 1620, 1411, and 1056 cm^{-1} were assigned to C = C/C = O, C-H, and C-O-C groups, respectively (Guo et al., 2023b; Kumar et al., 2023). The non-acidic groups (C = O and C-O-C) could favor MFC performance by significantly enhancing electron transfer activity, which were more abundant in SB (Zhong et al., 2019). It was suggested that SB likely enhanced denitrification and power generation in MFC-CW by improving the electron transfer process. Furthermore, SB exhibited a distinct peak at 590 cm^{-1}, attributed to the stretching vibration of the Fe-O bond, which was aligned with the EDS results (Li et al., 2024).

XPS was used to further understand the surface chemical composition of AC and SB. As shown in Fig. 2d, both carbon-based materials contained carbon and oxygen. In addition, SB contained elements such as iron, nitrogen, calcium, silicon, and aluminum, consistent with the EDS results (Fig. 2b). The C 1 s spectrum was displayed in Fig. 2e, assigned peaks at 284.8 eV, 286.6 eV, and 288.8 eV to C-C, C-O, and C = O, respectively. SB exhibited higher C-O and C = O peak areas, which agreed with the FT-IR results. Fig. 2f shows the Fe 2p, identifying peaks at 711.1 eV, 716.3 eV, 724.0 eV, and 728.9 eV as Fe 2p3/2, Fe 2p3/2, Fe 2p1/2, and Fe 2p1/2, respectively. This indicated the SB surface contained Fe^{2+} and Fe^{3+} forming iron compounds (Zhang et al., 2024a; Moradian et al., 2022). Additionally, the characteristic peaks of the N 1 s spectrum of SB (Fig. 2g) were deconvoluted into Pyridinic-N (398.1 eV), Pyrrolic-N (399.5 eV) and Graphitic-N (400.8 eV) (Zhong et al., 2019). Notably, Pyridinic-N and Graphitic-N play vital roles in ORR, providing active sites and reducing mass transfer resistance. Pyridinic-N could accelerate the oxygen reduction process by weakening the O-O bond, while Graphitic-N strengthens electrocatalytic properties by increasing conductivity in high-energy band domains (Ma et al., 2018). Furthermore, the degree of graphitization and defects in the carbon-based materials was assessed by the intensity ratio (I_D/I_G) from the Raman spectrum (Fig. 2h and i) (Cançado et al., 2024). The results exhibited that the I_D/I_G value of SB (0.95) was lower than that of AC (0.98), suggesting that SB was converted from amorphous carbon to ordered SP^2 microcrystals during pyrolysis with a higher degree of graphitization (Zheng et al., 2022). Besides, as illustrated in Fig. 2j, the CV curve of SB observed a substantial oxygen reduction process in an oxygen-saturated solution, whereas AC showed almost no reduction current. This indicated that SB had higher ORR catalytic activity than AC due to the higher content of metal and N-containing functional groups in SB, introducing defective sites and structural distortions (Zhang et al., 2024a).

In addition, Table S4 and Fig. S6 presented the physical properties of the two carbon materials. Specifically, SB exhibited higher hydrophilicity than AC, favoring bacterial attachment and thus enhancing denitrogenation and power production (Jia et al., 2018). In contrast, AC had a larger pore volume and surface area than SB. Generally, a larger pore volume and specific surface area favor nutrient capture and organic pollutant removal. To put it another way, it was suggested that pore volume and specific surface area were not the reasons for the enhanced nitrogen removal and electricity production by SB. Additionally, after 72 h of immersion in neutral pure water, the pH values of SB and AC were 7.73 and 9.04, respectively. Table S5 provided the DO and pH values recorded during the operation of each constructed wetland, with the pH ranging from 7.5 to 8.5. Previous studies indicate that bioelectricity generation and pollutant removal in MFC-CW systems are most efficient under slightly neutral to alkaline conditions (Doherty et al., 2015; Wang et al., 2016). These findings support the suitability of both AC and SB as

electrode materials for MFC-CW.

3.3. Carbon source release and electron transfer activity

Dissolved organic carbon (DOC) release was analyzed using deionized water extraction at 20 °C, and the average DOC content of SB (69.05 mg g^{-1}) was higher than that of AC (4.07 mg g^{-1}). In addition, the specific ultraviolet absorbance ($SUVA_{254}$) and bioavailability (optical indices such as slope ratio, S_R) values for dissolved organic matter (DOM) released from carbon materials was showed in Fig. 3a. The $SUVA_{254}$ value of AC (5.78 L mg^{-1C} m^{-1}) was much higher than SB (0.77 L mg^{-1C} m^{-1}), indicating that the DOM released from AC contained more aromatic organic matter. Higher S_R values reflect a lower relative molecular mass of released DOM, with SB at 8.94 ± 0.25 and AC at 2.92 ± 0.69. These results suggested that the DOM released by AC was more aromatic and had a higher molecular weight, making it harder for microorganisms to assimilate and utilize. Furthermore, the biodegradation index (BIX), humification index (HIX), and fluorescence index (FI) of EEM are depicted in Fig. 3b–d. The results suggested the greater bioavailability of the released DOM from SB. A high HIX value of AC means that the DOM is stable and humic in structure, making it hard utilize by microorganisms.

In addition, the fluorescence components (C1, C2, C3) of all extracted samples were analyzed by PARAFAC and shown in Fig. S7. C1 is typically considered a low molecular weight UVA humic-like compound (Burrows et al., 2013), C2 a protein-like component (Kothawala et al., 2012), and C3 a combined component containing both humic-like and protein-like DOM (Yang et al., 2013). Fig. 3e presented the significantly different fluorescence intensities of all components released by AC and SB in deionized water. Notably, the C1 and C2 fluorescence intensities of SB were 7.38 R.U. and 6.07 R.U., respectively, higher than those of AC (1.62 R.U. and 0.0018 R.U.). In addition, C1 and C2 occupied 75.66 % and 27.91 % of SB and AC, respectively (Fig. 3f). These results indicated that SB has a higher concentration of DOM and consists mainly of humic-like and protein-like compounds easier for microorganisms to utilize (Zheng et al., 2022). Furthermore, protein-like components could promote microbial activity to enhance denitrification performance (Zhou et al., 2024). Thus, SB could increase microbial abundance and activity by providing bioavailable carbon, facilitating pollutant removal and energy production.

Moreover, the denitrification process is an electron-driven biochemical reaction (Zheng et al., 2022). The microbial electron transport system activity (ETSA) were further analyzed for explaining the SB-enhanced nitrogen metabolism process. As shown in Fig. 3g, the average ETSA values for SBS-CW, MAC-CW, and MSBS-CW were 0.36, 0.31, and 0.58 μg O_2 g^{-1} $protein^{-1}$ min, respectively. A lower ETSA negatively affects the electron reduction reaction, resulting in lower bioelectricity production (Ji et al., 2022). This could explain the higher energy production in MSBS-CW.

3.4. Structure of microbial communities

The high-throughput sequencing was performed to elucidate the effects of different electrode materials and run modes on microbial community structure (Figs. 4, Fig. S8 and Table S6). Venn diagrams for each sample were presented in Fig. S8 to evaluate the distribution of OTUs across samples. A total of 6318 OTUs were identified from six groups of biofilm samples, among which 390 OTUs were shared, representing 6.17 % of the total. That suggested significant differences in the microbial community composition among the six groups. Moreover, the alpha diversity of the microorganisms was presented in Table S6 and the coverage of all samples exceeded 99 %, indicating that the results were reliable and representative. The cathode layer of each system had higher abundance (ACE and Chao 1) and diversity (Simpson and Shannon) than the anode layer (Xu et al., 2018). Furthermore, the order of microbial richness and diversity among different CW systems was MSBS-CW > SBS-CW > MAC-CW. It was showed that both SB and MFC could improve the microbial community structure of CWs.

In addition, the structure of microbial communities at the phylum and genus levels was illustrated in Fig. 4, in which A and C represent samples from the anode and cathode regions, respectively. At the phylum level (Fig. 4a), the dominant microbial populations were *Proteobacteria, Chloroflexi, Bacteroidota, Nitrospirota, Planctomycetota, Acidobacteriota, and Patescibacteria*. Among them, *Proteobacteria* had the highest relative abundance in each system (28.50 % - 45.19 %), generally associated with carbon and nitrogen cycling in wastewater treatment systems and playing essential roles in bioelectricity generation (Li et al., 2024). Notably, the phylum of *Chloroflexi* and *Bacteroidota* were involved in the degradation of complex organic matter (Li et al., 2023; Zhou et al., 2024).It was showed higher abundance in the anode layers than cathode layers in this study, indicating that organic matter consumption occurs mainly in the anode layer. *Chloroflexi* was more abundant (22.09 %) in MAC.A, which might contribute to the better COD removal in MAC-CW. The phylum of *Desulfobacterota* had high abundance (6.51 %) in MSBS.C, identified as an electroactive-rich bacterium (Zhu et al., 2022a), leading to increased power output in MSBS-CW. Furthermore, *Planctomycetota*, associated with aerobic heterotrophic and anaerobic denitrification (Tao et al., 2022b). It had the high relative abundance in MSBS-CW (4.30 % - 6.21 %) and SBS-CW (3.44 % - 4.36 %), suggesting that SB probably enhanced the anaerobic ammonium oxidation pathway.

To better understand the microbial community composition, Fig. 4b was displayed the shows distribution at the genus level. *Nitrospira, Candidatus_Competibacter, Dechloromonas, Stenotrophobacter*, and *Thauera* were the main genera in all systems. *Dechloromonas* and *Thauera* are typical heterotrophic denitrifying genus (Tao et al., 2022b; Zheng et al., 2022). SBS.A (4.35 %, 6.74 %), MAC.A (6.90 %, 5.16 %), MSBS.A (8.12 %, 2.96 %), SBS.C (10.17 %, 3.31 %), MAC.C (10.81 %, 3.79 %), and MSBS.C (13.47 %, 1.56 %) all had a high abundance, indicating that the heterotrophic denitrification process was present in all CW systems. C*andidatus_Competibacter* is a representative genus for COD and phosphorus removal (Shi et al., 2022). Its highest relative abundance in MAC-A (24.54 %) could explain the high COD removal at the MAC-CW. Notably, the microbial community structure of MSBS.C underwent significant changes. The MSBS.C had the highest abundance of *Geobacter* (10.81 %) compared to other samples (0.32 % - 1.70 %). *Geobacter* is a typical electroactive bacterium that forms conductive biofilm for rapid extracellular electron transfer (Gupta et al., 2023). The Fe (III) oxide and Graphitic - N on the SB surface favored the growth of *Geobacter*, thereby increasing the energy output (Zhang et al., 2024a). *Thiobacillus* was more abundant in MSBS.C (7.30 %) and SBS.C (1.67 %) than in the other samples (0.25 %−0.41 %), which is a Fe-based autotrophic denitrifying bacterium that could absorb electrons directly from the electrode to reduce NO_3^- (Shi et al., 2022; Xu et al., 2017). In addition, *Hydrogenophaga*, a hydrogen autotrophic denitrifying bacterium (Fan et al., 2022; Y. 2024). It had a higher relative abundance in MSBS.C (4.56 %) than in other samples (0 %−0.48 %). The above results suggested that SB enhanced the autotrophic denitrification process at the MFC-CW cathode. *Candidatus_Brocadia*, a typical genus of anaerobic ammonium oxidation bacteria, is an autotrophic bacterium that uses ammonia as an electron donor and nitrite as an electron acceptor to achieve nitrogen removal (Chen et al., 2020; Tao et al., 2022a). The relative abundance of *Candidatus_Brocadia* was higher in MSBS.A (4.10 %) and SBS.A (3.10 %) than in MAC.A (0.24 %), providing strong evidence that SB enhanced the anaerobic ammonium oxidation process in the anode layer.

The clustering analyses at the phylum and genus levels were performed to further analyze the impact of SB on microbial communities in MFC-CW (Fig. 4c and d). The clustering tree divided the samples into three main groups at the phylum and genus levels. One group contained SBS.C, MAC.A, and MAC.C; another group included SBS.A, MSBS.A; and the last group included only MSBS.C. As the system was open-circuited, SB altered the microbial community distribution in the anode.

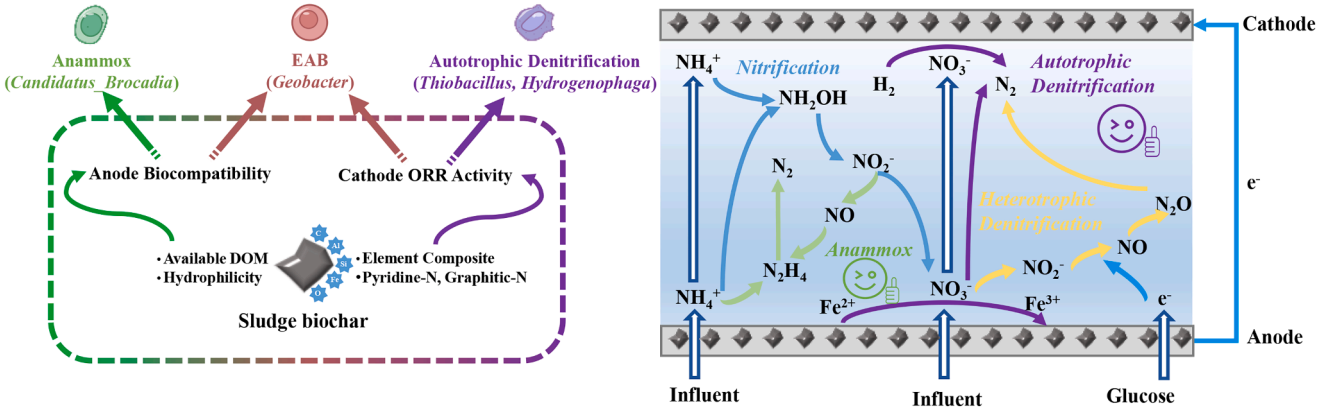

Fig. 5. Schematic diagram of the sludge biochar enhancement mechanism.

Interestingly, MSBS.C formed different microbial community structures from the other samples, suggesting that MFC could modify the cathode microbial structure in SB-based CW. Therefore, using SB as an MFC-CW electrode could improve the microbial community structure at both the cathode and anode, enhancing denitrification and energy output.

3.5. Enhancement mechanism of sludge biochar as electrodes

To explore the alteration of functional microorganisms by SB in MFC-CW, nitrogen functional genes were quantified (Fig. 4e). MSBS-CW showed the highest abundance of nitrification-related genes (nxrA: 2.32 × 10–5 - 7.65 × 10–5 %, amoB: 0.078 - 0.14 %, amoA: 0.20 - 0.27 %, hao: 0.0020 - 0.0043 %), suggesting that SB could enhance nitrification as an electrode. Similarly, denitrification-related genes (narG, nosZ, nirK, nirS) were more abundant in MSBS-CW than in other samples, indicating more complete denitrification. However, SBS-CW had the lowest abundance of denitrification genes, showing that MFC efficiently promoted denitrification. These results suggested that the synergistic interaction between SB and MFC contributed to the higher abundance of nitrogen-functional genes. Additionally, hzsB and hzo were typical functional genes for anaerobic ammonium oxidation (Wang et al., 2022a). SBS-CW (0.040 - 0.15 %) and MSBS-CW (0.10 - 0.23 %) had higher hzsB abundance compared to MAC-CW (0.0015 - 0.0060 %). Moerover, hzo was detected only in SBS-CW and MSBS-CW, corresponding to the higher abundance of *Candidatus_Brocadia* in high-throughput sequencing results.

According to the results, MSBS-CW demonstrated superior denitrification and power generation performance in carbon-constrained environments and the specific enhancement mechanism was depicted in Fig. 5. Iron and heteroatoms on the SB surface enhance ORR catalytic activity at the cathode layer and serve as electronic mediators for autotrophic denitrification. SB surfaces contained more Pyridinic-N, Graphitic-N, C = O, and C-O groups, facilitating ORR and electron transfer processes. Additionally, the more hydrophilic SB provided available carbon sources, enhancing biocompatibility and allowing microorganisms to better adapt to wetland environments in low-carbon conditions. Graphite-N and Fe (III) oxides on the material enriched *Geobacter* abundance, thereby promoting energy yield. This electron transfer from the anode to the cathode promoted autotrophic denitrification, increasing nitrogen removal. Furthermore, SB's biocompatibility and enhanced electron transfer activity could improve the anaerobic ammonium oxidation process in CW. Notably, autotrophic denitrification and anaerobic ammonium oxidation do not require an organic carbon source as an electron donor, providing a new solution to improve the nitrogen removal performance of CW in low-carbon conditions. Meanwhile, MFC-CW systems can effectively remove emerging pollutants, including pharmaceuticals, pesticides, and antibiotics (Liu et al., 2020). MSBS-CW demonstrated a more efficient bio-electrochemical process, which can enhance the removal rate of emerging contaminants (Luo et al., 2009). That provides a novel approach for the enhanced pollutants treatment in low-carbon wastewater.

4. Conclusions

This study verified the potential of sludge biochar (SB) and commercial activated carbon (AC) as electrodes for Microbial Fuel Cells - Constructed Wetlands (MFC-CW) in carbon-constrained environments, and explored the enhancement mechanism. Three sets of MFC-CWs were constructed: SB open circuit CW (SBS-CW), SB closed circuit CW (MSBS-CW), and AC closed circuit CW (MAC-CW). The results indicated that SB was more suitable than AC as an electrode material for MFC-CW under carbon-constrained conditions, achieving 90.59 % average TN removal and 9.05 mW m^{-2} maximum power density, significantly higher than MAC-CW. Material surface properties described by XPS, FT-IR, EDS, and electrochemical analysis suggested that SB effectively promotes ORR catalytic and electron transfer activity. Meanwhile, EEM and PARAFAC analyses indicated that SB-released DOM facilitated carbon source replenishment and microorganism adaptation, enhancing nitrogen removal. 16sRNA sequencing revealed that the SB-based MFC-CW was enriched with autotrophic denitrifying and anaerobic ammonium oxidation bacteria due to SB enhancing cathode ORR catalytic activity and anode biocompatibility. Correspondingly, nitrogen metabolism functional genes (hzsB, hzo, nirS, nikK, nosZ, etc.) had higher abundance in MSBS-CW. Overall, this study confirmed the efficacy of SB as an MFC-CW electrode in low-carbon environments, providing a reference for practical engineering applications and offering a new approach for municipal sludge recycling and reuse. However, the feasibility of large-scale construction needs further assessment to promote the application of reclaimed water treatment.

CRediT authorship contribution statement

Boda Ouyang: Writing – original draft, Visualization, Investigation, Formal analysis, Conceptualization. **Zhiyong Zhang:** Writing – review & editing, Project administration, Methodology, Conceptualization, Resources. **Fuzhi Chen:** Investigation. **Fei Li:** Supervision. **Ming-Lai Fu:** Writing – review & editing, Methodology, Conceptualization. **Huachun Lan:** Methodology. **Baoling Yuan:** Writing – review & editing, Supervision, Resources, Funding acquisition.

Declaration of competing interest

The authors declare that they have no known competing financial interests or personal relationships that could have appeared to influence the work reported in this paper.

Acknowledgments

This study was supported by the Major Program of National Natural Science Foundation of China (52293444), the Joint Funds of the National Natural Science Foundation of China (U24A20186), and the National Natural Science Foundation of China (52400044).

Supplementary materials

Supplementary material associated with this article can be found, in the online version, at doi:10.1016/j.watres.2024.123024.

Data availability

Data will be made available on request.

References

Burrows, R.M., Fellman, J.B., Magierowski, R.H., Barmuta, L.A., 2013. Allochthonous dissolved organic matter controls bacterial carbon production in old-growth and clearfelled headwater streams. Freshw. Sci. 32, 821–836. https://doi.org/10.1899/12-163.1.

Cançado, L.G., Monken, V.P., Campos, J.L.E., Santos, J.C.C., Backes, C., Chacham, H., Neves, B.R.A., Jorio, A., 2024. Science and Metrology of defects in graphene using Raman Spectroscopy. Carbon N.Y. 220, 118801. https://doi.org/10.1016/j.carbon.2024.118801.

Chen, W., Chen, S., Hu, F., Liu, W., Yang, D., Wu, J., 2020. A novel anammox reactor with a nitrogen gas circulation: performance, granule size, activity, and microbial community. Environ. Sci. Pollut. Res. 27, 18661–18671. https://doi.org/10.1007/s11356-020-08432-w.

Chen, Yiting, Yan, J., Chen, M., Guo, F., Liu, T., Chen, Yi, 2022. Effect of wetland plant fermentation broth on nitrogen removal and bioenergy generation in constructed wetland-microbial fuel cells. Front. Environ. Sci. Eng. 16, 157. https://doi.org/10.1007/s11783-022-1592-x.

Doherty, L., Zhao, Y., Zhao, X., Hu, Y., Hao, X., Xu, L., Liu, R., 2015. A review of a recently emerged technology: constructed wetland – microbial fuel cells. Water Res. 85, 38–45. https://doi.org/10.1016/j.watres.2015.08.016.

Ebrahimi, A., Sivakumar, M., McLauchlan, C., 2021. A taxonomy of design factors in constructed wetland-microbial fuel cell performance: a review. J. Environ. Manage. 291, 112723. https://doi.org/10.1016/j.jenvman.2021.112723.

El Barkaoui, S., Mandi, L., Aziz, F., Del Bubba, M., Ouazzani, N., 2023. A critical review on using biochar as constructed wetland substrate: characteristics, feedstock, design and pollutants removal mechanisms. Ecol. Eng. 190, 106927. https://doi.org/10.1016/j.ecoleng.2023.106927.

Fan, X., Li, J., He, L., Wang, Y., Zhou, Jiong, Zhou, Jian, Liu, C., 2022. Co-occurrence of autotrophic and heterotrophic denitrification in electrolysis assisted constructed wetland packing with coconut fiber as solid carbon source. Chemosphere 301, 134762. https://doi.org/10.1016/j.chemosphere.2022.134762.

Fan, Y., Sun, S., Gu, X., Zhang, M., Peng, Y., Yan, P., He, S., 2024. Boosting the denitrification efficiency of iron-based constructed wetlands in-situ via plant biomass-derived biochar: intensified iron redox cycle and microbial responses. Water Res. 253, 121285. https://doi.org/10.1016/j.watres.2024.121285.

Feng, H., Jia, Y., Shen, D., Zhou, Y., Chen, T., Chen, W., Ge, Z., Zheng, S., Wang, M., 2018. The effect of chemical vapor deposition temperature on the performance of binder-free sewage sludge-derived anodes in microbial fuel cells. Sci. Tot. Environ. 635, 45–52. https://doi.org/10.1016/j.scitotenv.2018.04.124.

Feng, L., Gao, Z., Hu, T., He, S., Liu, Y., Jiang, J., Zhao, Q., Wei, L., 2023a. Performance and mechanisms of biochar-based materials additive in constructed wetlands for enhancing wastewater treatment efficiency: a review. Chem. Eng. J. 471, 144772. https://doi.org/10.1016/j.cej.2023.144772.

Feng, L., Gao, Z., Hu, T., He, S., Liu, Y., Jiang, J., Zhao, Q., Wei, L., 2023b. Performance and mechanisms of biochar-based materials additive in constructed wetlands for enhancing wastewater treatment efficiency: a review. Chem. Eng. J. 471, 144772. https://doi.org/10.1016/j.cej.2023.144772.

Guo, F., Luo, Y., Nie, M., Zheng, F., Zhang, G., Chen, Y., 2023a. A comprehensive evaluation of biochar for enhancing nitrogen removal from secondary effluent in constructed wetlands. Chem. Eng. J. 478, 147469. https://doi.org/10.1016/j.cej.2023.147469.

Guo, F., Luo, Y., Nie, W., Xiong, Z., Yang, X., Yan, J., Liu, T., Chen, M., Chen, Y., 2023b. Biochar boosts nitrate removal in constructed wetlands for secondary effluent treatment: linking nitrate removal to the metabolic pathway of denitrification and biochar properties. Bioresour. Technol. 379, 129000. https://doi.org/10.1016/j.biortech.2023.129000.

Gupta, S., Patro, A., Mittal, Y., Dwivedi, S., Saket, P., Panja, R., Saeed, T., Martinez, F., Yadav, A.K., 2023. The race between classical microbial fuel cells, sediment-microbial fuel cells, plant-microbial fuel cells, and constructed wetlands-microbial fuel cells: applications and technology readiness level. Sci. Tot. Environ. 162757. https://doi.org/10.1016/j.scitotenv.2023.162757.

Ji, B., Zhao, Y., Yang, Y., Tang, C., Dai, Y., Zhang, X., Tai, Y., Tao, R., Ruan, W., 2022. Insight into the performance discrepancy of GAC and CAC as air-cathode materials in constructed wetland-microbial fuel cell system. Sci. Tot. Environ. 808, 152078. https://doi.org/10.1016/j.scitotenv.2021.152078.

Jia, Y., Feng, H., Shen, D., Zhou, Y., Chen, T., Wang, M., Chen, W., Ge, Z., Huang, L., Zheng, S., 2018. High-performance microbial fuel cell anodes obtained from sewage sludge mixed with fly ash. J. Hazard. Mater. 354, 27–32. https://doi.org/10.1016/j.jhazmat.2018.04.008.

Kothawala, D.N., von Wachenfeldt, E., Koehler, B., Tranvik, L.J., 2012. Selective loss and preservation of lake water dissolved organic matter fluorescence during long-term dark incubations. Sci. Tot. Environ. 433, 238–246. https://doi.org/10.1016/j.scitotenv.2012.06.029.

Kumar, A., Pandit, S., Sharma, K., Mathuriya, A.S., Prasad, R., 2023. Evaluation of bamboo derived biochar as anode catalyst in microbial fuel cell for xylan degradation utilizing microbial co-culture. Bioresour. Technol. 390, 129857. https://doi.org/10.1016/j.biortech.2023.129857.

Li, C., Feng, L., Lian, J., Yu, X., Fan, C., Hu, Z., Wu, H., 2023. Enhancement of organics and nutrient removal and microbial mechanism in vertical flow constructed wetland under a static magnetic field. J. Environ. Manage. 330, 117192. https://doi.org/10.1016/j.jenvman.2022.117192.

Li, Y., Tang, Y., Wu, Q., He, Y., Liu, Z., Yuan, S., Cheng, Q., Lian, X., Tan, Y., Su, Y., Chen, Y., 2024. Synergism of nitrogen removal and greenhouse gases emission reduction in pyrite/biochar-based bioretention system coupled with microbial fuel cell: performance and mechanism. J. Clean. Prod. 434, 140420. https://doi.org/10.1016/j.jclepro.2023.140420.

Liao, Y., Qiu, B., Hu, Q., 2023. The enhancement of nutrients removal performance in a vertical up-flow constructed wetland system using iron-carbon substrates. J. Environ. Chem. Eng. 11, 110036. https://doi.org/10.1016/j.jece.2023.110036.

Liu, Xianjing, Liang, C., Liu, Xiaohui, Lu, S., Xi, B., 2020. Intensified pharmaceutical and personal care products removal in an electrolysis-integrated tidal flow constructed wetland. Chem. Eng. J. 394, 124860. https://doi.org/10.1016/j.cej.2020.124860.

Liu, Y., Liu, X., Lu, S., Li, F., Wu, F., 2023. The difference between bioelectricity and direct current on the simultaneous removal of antibiotics and nitrogen in constructed wetlands. Chem. Eng. J. 475, 146499. https://doi.org/10.1016/j.cej.2023.146499.

Lu, R., Zhang, Q., Chen, Y., An, H., Zhang, L., Wu, Z., Xiao, E., 2024. Nitrate reduction pathway of iron sulphides based MFC-CWs purifying low C/N wastewater: competitive mechanism to inorganic and organic electrons. Chem. Eng. J. 479, 147379. https://doi.org/10.1016/j.cej.2023.147379.

Luo, H., Liu, G., Zhang, R., Jin, S., 2009. Phenol degradation in microbial fuel cells. Chem. Eng. J. 147, 259–264. https://doi.org/10.1016/j.cej.2008.07.011.

Ma, Jun, Xiao, D., Chen, C.L., Luo, Q., Yu, Y., Zhou, J., Guo, C., Li, K., Ma, Jie, Zheng, L., Zuo, X., 2018. Uric acid-derived Fe3C-containing mesoporous Fe/N/C composite with high activity for oxygen reduction reaction in alkaline medium. J. Power Source. 378, 491–498. https://doi.org/10.1016/j.jpowsour.2017.11.091.

Mian, M.M., Alam, N., Ahommed, M.S., He, Z., Ni, Y., 2022. Emerging applications of sludge biochar-based catalysts for environmental remediation and energy storage: a review. J. Clean. Prod. 360, 132131. https://doi.org/10.1016/j.jclepro.2022.132131.

Mian, M.M., Liu, G., Fu, B., 2019. Conversion of sewage sludge into environmental catalyst and microbial fuel cell electrode material: a review. Sci. Tot. Environ. 666, 525–539. https://doi.org/10.1016/j.scitotenv.2019.02.200.

Moradian, J.M., Wang, S., Ali, A., Liu, J., Mi, J., Wang, H., 2022. Biomass-derived carbon anode for high-performance microbial fuel cells. Catalysts 12, 894. https://doi.org/10.3390/catal12080894.

Ouyang, B., Li, F., Zhang, Z., Xie, X., Chen, L., Sun, W., Fu, M.-L., Yuan, B., 2024. Magnetic modification of cerium organic frame materials to improve the phosphorus adsorption performance: modulating the valence state. J. Environ. Chem. Eng. 12, 113807. https://doi.org/10.1016/j.jece.2024.113807.

Pyo, M., Kim, D., Kim, H.S., Hwang, M.-H., Lee, S., Lee, E.-J., 2024. Sulfur powder utilization and denitrification efficiency in an elemental sulfur-based membrane bioreactor with coagulant addition. Water Res., 122882 https://doi.org/10.1016/j.watres.2024.122882.

Rashid, K., Aslam, M., Rácz, E., Nadeem, S., Khan, Z., Muhammad, N., Rashid, Z., Aljuwayid, A.M., Shahid, M.K., Irfan, M., 2024. Mesoporous silica-grafted deep eutectic solvent-based mixed matrix membranes for wastewater treatment: synthesis and emerging pollutant removal performance. Nanotechnol. Rev. 13, 20230213. https://doi.org/10.1515/ntrev-2023-0213.

Shi, Y., Liu, T., Yu, H., Quan, X., 2022. Enhancing anoxic denitrification of low C/N ratio wastewater with novel ZVI composite carriers. J. Environ. Sci. 112, 180–191. https://doi.org/10.1016/j.jes.2021.05.021.

Sun, Y., Chen, Z., Wu, G., Wu, Q., Zhang, F., Niu, Z., Hu, H.-Y., 2016. Characteristics of water quality of municipal wastewater treatment plants in China: implications for resources utilization and management. J. Clean. Prod. 131, 1–9. https://doi.org/10.1016/j.jclepro.2016.05.068.

Tang, C., Zhao, Y., Kang, C., Yang, Y., Morgan, D., Xu, L., 2019. Towards concurrent pollutants removal and high energy harvesting in a pilot-scale CW-MFC: insight into the cathode conditions and electrodes connection. Chem. Eng. J. 373, 150–160. https://doi.org/10.1016/j.cej.2019.05.035.

Tao, M., Jing, Z., Tao, Z., Luo, H., Zuo, S., Li, Y.-Y., 2022a. Efficient nitrogen removal in microbial fuel cell – constructed wetland with corncobs addition for secondary effluent treatment. J. Clean. Prod. 332, 130108. https://doi.org/10.1016/j.jclepro.2021.130108.

Tao, M., Kong, Y., Jing, Z., Jia, Q., Tao, Z., Li, Y.-Y., 2022b. Denitrification performance, bioelectricity generation and microbial response in microbial fuel cell – constructed wetland treating carbon constraint wastewater. Bioresour. Technol. 363, 127902. https://doi.org/10.1016/j.biortech.2022.127902.

Tao, M., Kong, Y., Cao, S., Jing, Z., Guan, L., Jia, Q., Li, Y.-Y., 2024. Constructed wetland – Microbial fuel cell (CW-MFC) packed with suspended fillers to enhance

denitrification with Acorus calamus biomass addition. Chem. Eng. J. 487, 150753. https://doi.org/10.1016/j.cej.2024.150753.
Teoh, T.-P., Ong, S.-A., Ho, L.-N., Wong, Y.-S., Lutpi, N.A., Tan, S.-M., Ong, Y.-P., Yap, K.-L., 2024. Discerning the effect of operating conditions on the improvement of up-flow constructed wetland-microbial fuel cell performance in treating mixed azo dyes wastewater and bioelectricity generation. Energ. Ecol. Environ. 9, 301–313. https://doi.org/10.1007/s40974-023-00314-4.
Venâncio, J.P.F., Ribeirinho-Soares, S., Lopes, L.C., Madeira, L.M., Nunes, O.C., Rodrigues, C.S.D., 2023. Disinfection of treated urban effluents for reuse by combination of coagulation/flocculation and Fenton processes. Environ. Res. 218, 115028. https://doi.org/10.1016/j.envres.2022.115028.
Wang, J., Song, X., Wang, Y., Abayneh, B., Li, Y., Yan, D., Bai, J., 2016. Nitrate removal and bioenergy production in constructed wetland coupled with microbial fuel cell: establishment of electrochemically active bacteria community on anode. Bioresour. Technol. 221, 358–365. https://doi.org/10.1016/j.biortech.2016.09.054.
Wang, J., Sun, Y., Khunjar, W., Pace, G., McGrath, M., Chitrakar, S., Taylor, R.L., Carroll, J.R., Zhang, X., Wang, Z.-W., 2025. Mechanistic understanding of the performance difference between methanol- and glycerol-fed partial denitrification anammox in tertiary moving bed biofilm reactors treating real secondary effluent. Water Res. 271, 122893. https://doi.org/10.1016/j.watres.2024.122893.
Wang, W., Liu, Q., Xue, H., Wang, T., Fan, Y., Zhang, Z., Wang, H., Wang, Y., 2022a. The feasibility and mechanism of redox-active biochar for promoting anammox performance. Sci. Tot. Environ. 814, 152813. https://doi.org/10.1016/j.scitotenv.2021.152813.
Wang, Q., Lu, R., Yang, Y., Li, X., Chen, G., Shang, L., Peng, L., Sun-Waterhouse, D., Cowie, B.C.C., Meng, X., Zhao, Y., Zhang, T., Waterhouse, G.I.N., 2022b. Tailoring the microenvironment in Fe–N–C electrocatalysts for optimal oxygen reduction reaction performance. Sci. Bull. 67, 1264–1273. https://doi.org/10.1016/j.scib.2022.04.022.
Wei, Z., Yu, S., Shi, C., Li, C., 2024. Research progress of simultaneous nitrogen and phosphorus removal adsorbents in wastewater treatment. J. Environ. Chem. Eng. 12, 114844. https://doi.org/10.1016/j.jece.2024.114844.
Xu, Dan, Xiao, E., Xu, P., Lin, L., Zhou, Q., Xu, Dong, Wu, Z., 2017. Bacterial community and nitrate removal by simultaneous heterotrophic and autotrophic denitrification in a bioelectrochemically-assisted constructed wetland. Bioresour. Technol. 245, 993–999. https://doi.org/10.1016/j.biortech.2017.09.045.
Xu, F., Cao, F., Kong, Q., Zhou, L., Yuan, Q., Zhu, Y., Wang, Q., Du, Y., Wang, Z., 2018. Electricity production and evolution of microbial community in the constructed wetland-microbial fuel cell. Chem. Eng. J. 339, 479–486. https://doi.org/10.1016/j.cej.2018.02.003.
Yan, J., Hu, X., He, Q., Qin, H., Yi, D., Lv, D., Cheng, C., Zhao, Y., Chen, Y., 2021. Simultaneous enhancement of treatment performance and energy recovery using pyrite as anodic filling material in constructed wetland coupled with microbial fuel cells. Water Res. 201, 117333. https://doi.org/10.1016/j.watres.2021.117333.
Yang, L., Guo, W., Chen, N., Hong, H., Huang, J., Xu, J., Huang, S., 2013. Influence of a summer storm event on the flux and composition of dissolved organic matter in a subtropical river, China. Appl. Geochem. 28, 164–171. https://doi.org/10.1016/j.apgeochem.2012.10.004.
Yang, R., Liu, M., Yang, Q., 2022. Microbial fuel cell affected the filler pollution accumulation of constructed wetland in the lab-scale and pilot-scale coupling reactors. Chem. Eng. J. 429, 132208. https://doi.org/10.1016/j.cej.2021.132208.
Yuan, Y., Liu, T., Fu, P., Tang, J., Zhou, S., 2015. Conversion of sewage sludge into high-performance bifunctional electrode materials for microbial energy harvesting. J. Mater. Chem. A 3, 8475–8482. https://doi.org/10.1039/C5TA00458F.
Zhang, F., Shen, C., Zhao, Y., Zhang, S., Wang, Y., Ji, B., Liu, R., Hung Wong, M., Shan, S., Zhang, J., 2024a. An integrated constructed wetland-Microbial fuel cell system with sewage sludge-biochar to enhance treatment and energy recovery efficiencies. Chem. Eng. J. 486, 150431. https://doi.org/10.1016/j.cej.2024.150431.
Zhang, Z., Liu, C., Ouyang, B., Fu, M.-L., Xu, L., Lan, H., Yuan, B., 2024b. A systematic investigation of peracetic acid oxidation and polymeric coagulants re-flocculation to enhance activated sludge dewatering: multi-porous skeleton structures. J. Environ. Manage. 367, 121946. https://doi.org/10.1016/j.jenvman.2024.121946.
Zhao, F., Zhang, X., Xu, Z., Feng, C., Pan, W., Lu, L., Luo, W., 2024. Review of hydraulic conditions optimization for constructed wetlands. J. Environ. Manage. 370, 122377. https://doi.org/10.1016/j.jenvman.2024.122377.
Zheng, F., Fang, J., Guo, F., Yang, X., Liu, T., Chen, M., Nie, M., Chen, Y., 2022. Biochar based constructed wetland for secondary effluent treatment: waste resource utilization. Chem. Eng. J. 432, 134377. https://doi.org/10.1016/j.cej.2021.134377.
Zhong, K., Li, M., Yang, Y., Zhang, H., Zhang, B., Tang, J., Yan, J., Su, M., Yang, Z., 2019. Nitrogen-doped biochar derived from watermelon rind as oxygen reduction catalyst in air cathode microbial fuel cells. Appl. Energy 242, 516–525. https://doi.org/10.1016/j.apenergy.2019.03.050.
Zhou, C., Wu, J., Ma, W., Liu, B., Xing, D., Yang, S., Cao, G., 2022. Responses of nitrogen removal under microplastics versus nanoplastics stress in SBR: toxicity, microbial community and functional genes. J. Hazard. Mater. 432, 128715. https://doi.org/10.1016/j.jhazmat.2022.128715.
Zhou, T., Hu, W., Lai, D.Y.F., Yin, G., Ren, D., Guo, Z., Zheng, Y., Wang, J., 2024. Interaction of reed litter and biochar presences on performances of constructed wetlands. Water Res. 254, 121387. https://doi.org/10.1016/j.watres.2024.121387.
Zhu, K., Xu, Y., Yang, X., Fu, W., Dang, W., Yuan, J., Wang, Z., 2022a. Sludge derived carbon modified anode in microbial fuel cell for performance improvement and microbial community dynamics. Membrane. (Basel) 12, 120. https://doi.org/10.3390/membranes12020120.
Zhu, X., Shen, C., Huang, J., Wang, L., Pang, Q., Peng, F., Hou, J., Ni, L., He, F., Xu, B., 2022b. The effect of sulfamethoxazole on nitrogen removal and electricity generation in a tidal flow constructed wetland coupled with a microbial fuel cell system: microbial response. Chem. Eng. J. 431, 134070. https://doi.org/10.1016/j.cej.2021.134070.
Zhuang, L.-L., Li, M., Li, Y., Zhang, L., Xu, X., Wu, H., Liang, S., Su, C., Zhang, J., 2022. The performance and mechanism of biochar-enhanced constructed wetland for wastewater treatment. J. Water Process Eng. 45, 102522. https://doi.org/10.1016/j.jwpe.2021.102522.